The Solar Polar Orbiter: A Solar Sail Technology Reference Study

Malcolm Macdonald,[†] Gareth W. Hughes,[‡]

University of Glasgow, Glasgow, Scotland.

Colin R M[c]Innes,[§]

University of Strathclyde, Glasgow, Scotland.

Aleksander Lyngvi,[**] Peter Falkner,[**] Alessandro Atzei[**]

European Space Agency, Noordwijk, The Netherlands.

Abstract

This paper presents an assessment of a Solar Polar Orbiter mission as a Technology Reference Study. The goal is to focus the development of strategically important technologies of potential relevance to future science missions. In this paper the technology is solar sailing, so the use of solar sail propulsion is thus defined a priori. The primary mission architecture utilizes maximum Soyuz Fregat 2-1b launch energy, deploying the sail shortly after Fregat separation. The 153 × 153 m square sail then spirals into a circular 0.48 AU orbit, where the orbit inclination is raised to 90 deg `with respect to the solar equator in just over 5 years. Both the solar sail and

[†] Now at SciSys Ltd, Bristol, England.

malcolm.macdonald@scisys.co.uk

[‡] Research Assistant, Department of Aerospace Engineering.

[§] Professor, Department of Mechanical Engineering, Member AIAA

colin.mcinnes@strath.ac.uk

[**] Science Payload and Advanced Concepts Office, ESTEC

alyngvi@rssd.esa.int

spacecraft technology requirements have been addressed. The sail requires advanced boom and new thin-film technology. The spacecraft requirements were found to be minimal, as the spacecraft environment is relatively benign in comparison with other currently envisaged missions, such as the Solar Orbiter mission and BepiColombo.

Introduction

The Science Payload and Advanced Concepts Office of ESA (European Space Agency) have introduced Technology Reference Studies (TRS) to focus the development of strategically important technologies of likely relevance to future science missions. This is accomplished through the study of technologically demanding and scientifically interesting missions, which are not part of the ESA science programme. This paper discusses one such mission, the Solar Polar Orbiter (SPO). The TRS cover a wide range of mission profiles with an even wider range of strategically important technologies. All TRS mission profiles are based on small satellites, with miniaturized highly integrated payload suites, launched on a Soyuz Fregat 2-1b.[1]

Science missions are technologically very challenging. It is important to define and prepare critical technologies far in advance, hence ensuring they are developed in a timely manner and that associated cost, risk and feasibility of potential future mission concepts can be properly estimated. The TRS are set up to provide a set of realistic requirements for these technology developments far before specific science missions are proposed by the scientific community. Through their study a set of detailed requirements for technology development activities can be determined. The TRS are a tool to focus technology development activities; they are not part of ESA's science

mission programme. A TRS is carefully selected to address a wide range of technologies that have to be applicable to many other scientific mission profiles.

Terrestrial observations of the Sun are restricted to the ecliptic plane and within the solar limb, thus restricting observations to within ± 7.25 deg of the solar equator. Close solar measurements at all latitudes are necessary to achieve a global three-dimensional picture of solar features and processes. Observations directly over the solar poles are imperative to understanding the Sun. Most previous missions to study the Sun have been restricted to observations from within the ecliptic. The Ulysses spacecraft used a Jupiter gravity assist to pass over the solar poles, obtaining field and particle measurements but no images of the poles.[2] Furthermore the Ulysses orbit is highly elliptical; with a pole revisit time of approximately 6 years. It is desired that future solar analysis be performed much closer to the Sun, as well as from an out-of-ecliptic perspective. The Solar Orbiter mission scheduled for launch in October 2013 intends to deliver a science suite of order 180 kg to a maximum inclination of order 35 deg with respect to the solar equator and to a minimum solar approach radius of 0.22 AU using SEP (Solar Electric Propulsion).[3] The inability of the Solar Orbiter mission to attain a solar polar orbit highlights the difficulty of such a goal with conventional propulsion. A 1998 study considered the use of solar sail technology to place a science payload into a solar polar orbit.[4] Reference 4 defined a 164 kg spacecraft, using a 6 g m^{-2}, 158 × 158 m solar sail and a cruise time of 4.6 yrs. Within this prior study the definition of solar sail technology requirements is imprecise due to the technology status of solar sail hardware at the time.

The primary objective of the mission presented in this paper is to deliver a spacecraft into an orbit at 90 deg inclination with respect to the solar equator, using a launch vehicle no larger than the Soyuz Fregat 2-1b. The spacecraft orbit should be phased such that once on-station it will remain near to the solar limb from a terrestrial perspective. The spacecraft should also be positioned on an orbit interior to Earth's.

This paper summarizes the output from the SPO TRS, allowing definition of key technology requirements for this class of solar sail mission. The SPO TRS draws some significantly different conclusions from similar previous studies, many of which are due to the fundamentally different methodologies utilized; these will be discussed within this paper. In particular this paper develops the mission concept with realistic orbit trajectory generation to the actual science orbit rather than some approximation of this orbit. The SPO spacecraft systems are fully defined within the technology limits of the mission timeframe and with consideration of the limitations due to the use of solar sail propulsion, such as pointing accuracy due to sail flexing. The solar sail system and technology requirements are also fully defined. A full range of mission architectures have been investigated in order to ensure that an optimal reference mission is generated. Furthermore, the global effect of varying the solar close approach radius is considered for the first time through amalgamation of trajectory and spacecraft / sail systems into one complete analysis.

Top-Level Baseline Science Objectives

The many potential science objectives and goals of a SPO mission have previously been discussed in detail in Ref. 4. The purpose of this paper is to address the

technology goals and requirements of such a mission and as such discussion of science goals is limited to top-level baseline objectives.

The solar wind, in addition to higher energy solar flare particles, can induce power line surges and radio interference on the Earth, as well as causing the well known aurora borealis. Observations from Ulysses shows that the 11-year solar cycle minimum causes the solar wind speed at polar latitudes to almost double the equatorial value, from a speed of order 450 km s^{-1} to 750 km s^{-1}. The solar wind also appears to have a different composition at the solar poles. A close solar polar orbiter would thus enable further investigation into the polar solar wind data obtained by Ulysses and likely to be obtained from the Solar Orbiter mission over a range of inclinations up to 35 deg. Furthermore, it is important that we can obtain an understanding of the relationship between solar wind velocity and the solar magnetic field geometry, with the best location to accurately assess the longitudinal structure of the magnetic field in the corona being from polar latitudes. Solar polar observations would also address the scale over which the co-rotation of coronal plasma with the Sun is lost. Combined coronagraph data would thus allow the determination of three-dimensional structures and show the locations of streamers, rays, and plumes in the corona. Considerable fine structures, termed microstreams, were observed in high-speed flow from coronal holes at the poles by Ulysses. Relating the microstreams to polar plumes, supergranulation patterns and bright flares would be enabled by a spacecraft in a solar polar orbit.[4]

Mission Architecture

The mission is split into seven core phases, ranging from Launch through to sail jettison and the beginning of the science mission and then on into a potential extension to the science mission. The longest mission phase is the transfer trajectory, which is provisionally scheduled as 5 years, although this will vary depending on the final selected sail characteristic acceleration. We define characteristic acceleration as the acceleration the sail actually provides at a solar distance of 1 AU, with the sail normal to the Sun-line. Following the arrival of the spacecraft at the solar polar orbit the sail is jettisoned to allow the science operations phase to begin. The spacecraft attitude and orbit maintenance is from this point on performed using a hydrazine system as will be discussed later. Science operations are provisionally scheduled for 2 years. The target solar polar orbit is defined by the direction of the solar poles. Thus, the desired polar orbit is inclined at 82.75 deg with a right ascension of ascending node of 255.8 deg at J2000 (corresponding to the Julian day 2451545) with a drift rate of plus 0.014 deg yr^{-1}, within a standard ecliptic plane reference frame**.** Analysis of sunspots has revealed that the direction of the solar poles is less well defined than indicated above,[5] however we adopt these values as the target orbit. Spacecraft orbit phasing with respect to the Earth must be carefully considered. Science returns are maximized when the spacecraft is positioned near to the solar limb as seen from Earth, allowing observation of the corona along the Sun-Earth line. Maintaining this alignment eliminates solar conjunctions and hence loss of telemetry. It is thus considered necessary that the spacecraft orbit is in resonance with Earth's orbit about the Sun. Potential target solar orbits are defined as a circular polar orbit with radius $N^{-2/3}$ AU for integer values of N, where N is the orbit resonance number. Figure 1 illustrates the Earth – Sun – sail separation angle for $1 \leq N \leq 5$. It is seen that

as the orbit resonance number is increased the separation angle tends further from 90 deg, hence degrading mission science returns. At N = 1 the Earth – Sun – sail separation angle stays within ± 27 deg of 90 deg, while at N = 5 the Earth – Sun – sail separation angle peaks at over ± 73 deg from 90 deg. The choice of optimal resonant orbit depends on a number of factors. Far from the Sun, larger aperture instruments are required to maintain image resolution, with only infrequent passes over the solar pole. However, the Earth – Sun – sail separation angle stays close to 90 deg. Closer to the Sun we obtain frequent passes over the solar poles and very high resolution imaging, but the spacecraft thermal environment becomes increasingly severe, while also passing further from the solar limb. Thus, a balance must be sought based on spacecraft engineering constraints, cost and science goals. The N = 3 resonant orbit is defined as the target scientific orbit as this places the spacecraft close to the Sun, while also being in a relatively benign thermal environment compared to closer resonant orbits. This orbit also maintains the spacecraft within ± 30 deg of the solar limbs for the majority of the mission duration. Figure 1 also illustrates the trajectory of the solar polar orbit for N = 3. The trajectory is seen from an Earth-centered coordinate system, with the Sun fixed along the negative X axis. The asymmetry for N = 3 (and N = 1) can be reversed by a simple alteration of the initial conditions.

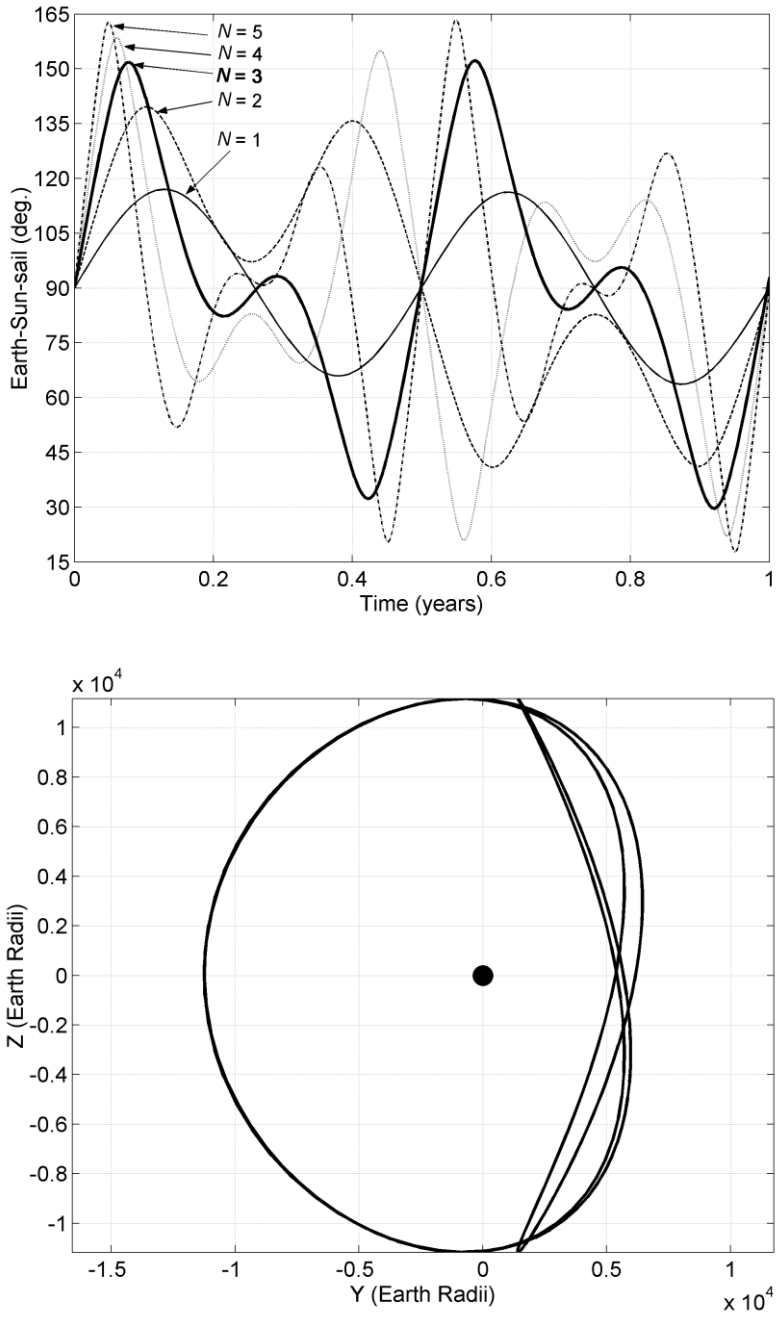

Figure 1 Earth – Sun – sail separation angle for $1 \leq N \leq 5$, top, and trajectory plot for $N = 3$ solar polar orbit in an Earth-centered rotating reference frame, bottom.

Spacecraft Model

Within this paper the term "spacecraft" means the vehicle which will perform the science operations at the defined target orbit and does not necessarily include the solar

sail. Conventionally this craft has been called the “solar sail payload” however the spacecraft will command and control the solar sail, which will not be capable of independent operation. The term spacecraft is thus more appropriate. The solar sail is a fully-integrated sub-system of the spacecraft, however for the purpose of technology definition requirements it is presented here as a separate entity.

Throughout the solar polar spacecraft design full redundancy is maintained, except for the high-gain antenna (HGA). We note further that many components of the solar sail, such as sail film, cannot be supported through redundancy due to mass and/or volume considerations however full redundancy is applied to the sail where possible. The spacecraft systems analysis is based on a minimum solar approach thermal limit of 0.48 AU, the baseline mission profile. However, an analysis will also be presented as to the effect of varying the thermal limit. An overview of the spacecraft mass budget is shown in Table 1 as part of a complete launch mass breakdown. We note that the total spacecraft wet mass is 247.9 kg, of which 41.2 kg consists of the science instrument allocation. Table 1 gives the current best estimate (CBE) mass which then has a design maturity margin (DMM) added to give the total sub-system mass allocation. The design maturity margin is added at equipment level, where > 5 % is added for off-the-shelf items (European Cooperation for Space Standardisation, ECSS, Category: A/B), > 10 % for off-the-shelf items requiring minor modifications (ECSS Category: C) and > 20 % is added for new design/development items, or items requiring major modifications or re-design (ECSS Category: D). We note in Table 1 that the added DMM can appear somewhat arbitrary. For example, the power sub-system DMM is 8.3 %. However, this is simply a result of averaging the DMMs allocated at the equipment level. We anticipate only limited technology issues with

the spacecraft sub-systems as the space environment at 0.48 AU is relatively benign in comparison with other currently envisaged missions, including BepiColombo[6] and the solar orbiter mission. Note however that direct adaptation of technology is rarely possible and thus some limited modifications and developments are inevitable.

Table 1 Mass budget, with scaling laws rounded to one decimal place.

System	CBE Mass	DMM	CBE Mass + DMM
Science Instruments	37.0 kg	10.8 %	41.2 kg
Attitude & Orbit Control System, AOCS (dry)	28.7 kg	5.0 %	30.1 kg
Telemetry, Tracking and Command, TT&C	48.3 kg	5.0 %	50.7 kg
On-Board Data Handling, OBDH	4.2 kg	10.0 %	4.7 kg
Thermal & Radiation	9.6 kg	10.0 %	10.6 kg
Power	42.9 kg	8.3 %	46.8 kg
Mechanisms & Structure	49.2 kg	7.5 %	53.0 kg
Spacecraft Nominal Dry Mass At Launch			237.1 kg
AOCS propellant, inc. sail separation allowance and a margin			10.8 kg
Spacecraft Nominal Wet Mass at Launch			247.9 kg
Solar Sail Nominal Mass at Launch (see also Table 5)			195.9 kg
Nominal Launch Mass			443.9 kg
ESA System Level Margin		20.0 %	88.8 kg
Total Mass At Launch			532.7 kg
Soyuz Fregat 2-1b launch capacity (C_3 = 38.84 km^2 s^{-2})			620.0 kg
Launch Margin			87.4 kg (14.1 %)

Science Instruments

During this TRS a representative set of instruments for the mission were defined, together with basic system-level requirements. Thus, a strawman payload was implemented to allow mission analysis. The current strawman payload comprises six instruments, detailed in Table 2. A relatively simple package of plasma instruments is required to relate the properties of the solar wind at 0.48 AU to the solar and coronal features studied with the remote sensing instruments. However, the spacecraft field must be low (preferably < 1 nT), known and constant so the magnetometer data can be corrected on-board and used in reducing the plasma distributions from the three-dimensional measured distributions to the two-dimensional, field-aligned distributions to be returned to Earth. A deployable 2.5-m boom from the spacecraft was selected.

Table 2 Strawman payload budget

Component	CBE Mass (kg)	DMM (%)	Total Mass (kg)	Average Power (W)
Coronagraph	10.0	10.0	11.0	10
Extreme Ultraviolet Imager	10.0	10.0	11.0	10
Velocity and Magnetograph Imager	10.0	15.0	11.5	10
Plasma Analyzer	3.0	10.0	3.3	4
Magnetometer	2.0	10.0	2.2	4
Energetic Particle Telescope	2.0	10.0	2.2	4

We recall the transfer trajectory mission phase lasts approximately 5 years. The mission can thus be significantly enhanced if the science suite can be utilized during this period, while the spacecraft retains the sail. Use of the science suite during the transfer trajectory would enable a full comparison of the solar environment at all latitudes. It is anticipated that the solar sail will have pointing accuracy of

approximately 1 deg due to sail flexing, while pointing knowledge of the science suite would be high as this can be determined by the spacecraft's attitude and orbit control system (AOCS). Pointing stability of the science suite is difficult to determine, although we note that the lowest structural mode frequency of a solar sail is typically below 0.1 Hz.[7, 8] It is thus feasible that while attached to the sail the pointing stability over very short integration times may be compatible with the required instrument stability, allowing some low quality data to be generated by the imaging instruments during the transfer trajectory through the use of shortened integration times. Note however, on-board autonomy would be required to select the images which are of scientific use as sail flexing means the instrument field-of-view may be sub-optimally orientated. The pointing requirements of the plasma analyzer and magnetometer match the sail design specifications, however it is unclear if the local spacecraft environment will be suitable for use of such instruments.[9] We note that the analysis within this paper assumes no science during the transfer trajectory.

Attitude and Orbit Control System

The AOCS is defined for the two distinct phases of being attached to the sail and then following sail jettison. The solar polar spacecraft is three-axis stabilized at all times, with a baseline pointing control of 360 arcseconds following sail jettison provided for the payload instruments that are considered to be always-on, such as the plasma analyzer and magnetometer. Higher, short term pointing stability is provided for the imagers. It was found that little gain was made by relaxing the nominal pointing requirement since the magnetometer has a required pointing stability of 360 arcseconds per second. Furthermore, maintaining pointing control at 360 arcseconds allows the X-Band HGA to be used at any time through the mission, for example in

space weather applications, with no impact on the AOCS hydrazine budget used for attitude control following sail jettison.

Pointing knowledge is maintained by a combination of coarse Sun sensors, gyroscopes and star sensors, while attached to the sail. Recall, the lowest structural mode frequency of a solar sail is typically below 0.1 Hz,[7, 8] thus as the sail flexes the orientation of the thrust vector is fairly uncertain and highly accurate guidance becomes difficult, meaning that the sail will require many course corrections over the period of the transfer trajectory due to thrust vector misalignment errors. Pointing knowledge is maintained by star sensors and gyroscopes once the sail has been jettisoned and continuing through the science operations phase. Reaction wheels, which are unloaded through the use of a monopropellant system, maintain spacecraft pointing stability. It is not possible to utilize all instruments all of the time due to pointing requirements, however we wish to maximize the use of all instruments. Analysis of propellant requirements leads to the conclusion that a hydrazine system is preferable to a cold-gas system due to the reduction in propellant mass. We note that part of the AOCS propellant mass budget is a contingency propellant budget which is provided for use in the sail separation and avoidance maneuver, the specifics of which will be discussed later within this paper. The AOCS propulsion assumes a specific impulse of 200 seconds for pulse maneuvers and 230 seconds for longer duration burns, such as the sail separation and avoidance maneuver. The AOCS propellant mass total is 10.8 kg, as seen in Table 1.

Telemetry, Tracking and Command (TT&C)

No significant technology requirements were identified within this sub-system. However, some important trades were required to define an optimal solution between sail and spacecraft requirements which vary the system design from a non-sail delivered solar polar orbiter spacecraft.

Data latency is nominally set at less than 1 week, which coupled with a continuous science data acquisition stream of 3.5 kbps means that we acquire approximately 2.1 Gbit of data between downlinks. Assuming each downlink is 8 hrs we can then define a required minimum science telemetry downlink rate of 73.5 kbps. Maximum slant range for the Science Operations mode is approximately 1.46 AU. At this slant range we find that the required spacecraft transmitter power is just over 28 W. Therefore, in order to provide a margin for return of engineering data at all times we set the spacecraft transmitter power at 30 W, giving a design telemetry rate (downlink) of 77.8 kbps and a command rate (uplink) of 38.9 kbps. The minimum margin for engineering data is 4.3 kbps, however this margin increases to over 386 kbps at the minimum slant range of 0.6 AU.

As discussed previously, the expected pointing accuracy while attached to the sail is low due to sail flexing, thus limiting communications to X-Band frequencies and lower while the spacecraft is attached to the sail. We can however consider adoption of a dual X and Ka-Band system which would allow increased data rates, reduced frequency of downlinks and a reduction in power requirements during the science phase of the mission, or a combination of each. Using a 35 m dish in the Ka-band, at 20 kW to match ESA ground station network (ESTRACK) configuration, and

increasing the spacecraft pointing accuracy during downlinks to 36 arcseconds, as required for Ka-band, we can analyze such an option. AOCS mass marginally increases assuming one 1.5 m HGA downlink of 8 hrs per week in a 2-year mission due to the increased pointing requirements. The spacecraft transmitting power can be significantly decreased during the Ka-Band HGA downlinks as the available command rate otherwise increases to over 8 Mbps and the telemetry rate to just less than 1 Mbps, assuming conditions such as antenna elevation and weather confidence are similar. However, in order to maintain sufficient link margins and data rates within the other communication modes, we require to maintain spacecraft transmitting power at 30 W within the X-Band limited modes of cruise and emergency, negating the potential power saving available during the science operations mode. Furthermore, during the science operations mode the spacecraft is in a power rich environment and thus power savings are not of significant benefit. We note however that adoption of Ka-Band within the science operations mode would allow a Solid State Power Amplifier (SSPA) to be flown, as spacecraft transmitting power requirements are only 5 W for one 8 hr downlink per week, allowing increased sub-system reliability at the expense of additional mass. It is found that the adoption of a dual X and Ka-band communications architecture, with SSPA, increases the spacecraft total mass by 6.4 kg, which in turn increases sail side length by almost 2 m and total mass at launch by 11.9 kg. The selected spacecraft communications architecture is limited to X-band frequencies, which reduces HGA surface tolerance design limits and removes any potential requirement for a two-way capable Ka-band small deep space transponder (SDST) as current SDST technology is limited to two-way X-band and downlink only in Ka-band.

Maintaining the spacecraft transmitting power at 30 W allows the calculation of the attainable data rates within the other communication modes. We see in Table 3 the available data rates in each communication mode, at the maximum design slant range. Each communication mode strives to minimize ground segment costs and requirements, hence utilizing as small a ground station as possible, as detailed in Table 3. Note the design HGA size is 1.5 m diameter.

Table 3 Available data rates, at the maximum design slant range defined by trajectory analysis

Communication Mode Name	Antenna – Ground Station	Mode Design Slant Range	Minimum Data Rate Command	Telemetry
Cruise	LGA – 15 m	1.80 AU	0.03 kbps	0.04 kbps
Space Weather	LGA – 5 m	1.46 AU	0.00 kbps	0.01 kbps
Science Operations	HGA – 35 m	1.46 AU	38.9 kbps	77.8 kbps
Emergency	LGA – 35 m	1.80 AU	0.03 kbps	0.21 kbps

The use of alternative ground stations would clearly allow for increased data rates, however sufficient data rates are attainable within each mode. It is considered optimal that data latency be set at the nominal value of 1 week, with a transmitter power rating of 30 W within all communication modes. Data can however be returned at increased frequencies and so the data latency setting is a nominal design value which is used to define on-board memory requirements within the data handling sub-system.

The 0.48 AU orbit is not ideal for dedicated Earth related space weather observations. However, the 0.48 AU orbit allows the observation of coronal mass ejections directed

towards Earth for much of the time. The instrumentation on-board can therefore provide an additional contribution to space weather forecasts. The spacecraft could provide up to a 1-day warning of large solar proton events. The space weather communication architecture selected within this paper is based on beacon-mode technology. A simple tonal system is used to indicate whether or not an event has occurred. The beacon mode requires an onboard system that can communicate with Earth 24-hours a day and at least 3 ground antenna, hence the selection of ESTRACK 5 m stations as shown in Table 3, which are currently available and would require minimal further investment. Upon detection of an event, emergency use of a 35 m ESTRACK antenna commands the spacecraft to transmit a special downlink load. The additional cost and system requirements for operating the beacon mode are included in the baseline mission.

Power

The power sub-system analysis suggests no significant technology issues that we cannot reasonably except to be solved within other currently active studies.[3, 6] We note however that design techniques, such as advanced computer aided design allow the reduction of harness mass through better design methodologies, such mass savings are significant for enhancing solar sailing missions. The power system is supplemented by Lithium Ion batteries, which are designed to carry the power load during the launch phase and to absorb peak power loads during other mission phases, for example during the transfer trajectory when sail pitch may limit array performance. The nominal power loads for solar array and battery sizing are defined in Table 4, where we see that the power load is split into three main categories. The design power load is defined as the nominal power load (Table 4) plus a 20 % system

level margin. Solar array design is based on Spectrolab 26.8 % Improved Triple Junction (ITJ) solar cells.[10] In order to maintain the solar array within thermal bounds it is found that at end-of-life (EOL) the array must be pitched at over 63 deg from the Sun-line. However, the use of Carbon – Carbon substrates, as in BepiColombo, may also prove beneficial. The total array surface area is found to be 1.03 m^2, which is divided into two wings. The small surface area required allows for simple planar arrays to be envisaged, without the need for them to unfold following spacecraft launch. We note that despite the increased solar flux at 0.48 AU the solar array design point was found to be at EOL due to array degradation during the mission, the significant thermal losses encountered at 0.48 AU and that the power load is highest during this mission phase. The cell efficiency at EOL is 19 %.

Table 4 Power Budget

System	Launch Power, Design Point 1 AU	Transfer Power, Design Point 0.48 AU	Science Power, Design Point 0.48 AU
Science Instruments	0.0 W	0.0W	24.7 W
AOCS	35.2 W	17.4W	47.8 W
TT&C	0.0 W	73.9W	73.9 W
OBDH	7.9 W	17.4W	26.1 W
Thermal & Radiation	83.1 W	83.6W	83.6 W
Power	35.4 W	27.0W	27.3 W
Mechanisms & Structure	0.0 W	4.2W	9.5 W
Solar Sail	0.0 W	10.9W	0.0 W
Nominal Power Load	161.6 W	234.4W	292.9 W

Remaining Spacecraft Sub-Systems

The on-board memory requirements are defined in part by the maximum data latency setting of one week, thus the spacecraft acquires just over 2 Gbit of data between downlinks. Furthermore, it is required that the solar sail be highly autonomous, necessitating sizeable computational and storage capabilities.

Within the remaining sub-systems no significant technology issues were identified within this analysis. Note that the placement of the spacecraft within the plane of the sail film means that the heat generated by the sail, both reflected and emitted, has a very low view factor with respect to the spacecraft systems. Thus the sail thermal input to the spacecraft is negligible. An initial radiation analysis suggested a conservative design tolerance of 75 krad should be adopted.

The spacecraft configuration is assumed to be a cube of sides 1.1 m. We note however from the solar orbiter mission studies that the spacecraft thermal design may be aided by adoption of a rectangular design rather than a cube. Figure 2 shows a visualization of the SPO spacecraft in deployed configuration, allowing the volumetric requirements of the spacecraft to be analyzed and aiding in the launch vehicle configuration analysis later within this paper. The imaging science instruments are mounted internally, with field-of-view towards the Sun along the negative X-axis, this provides a clear field-of-view as the face is maintained in a sunward orientation through bias torque. A 2-axis steerable HGA is mounted on the anti-Sun side, the positive X-axis, so the HGA is provided with a degree of thermal protection due to the shadow from the main spacecraft body. However, in this initial configuration there is potential for the (hot) solar arrays to impinge the field-of-view

of the HGA. Two sets of one degree of freedom steerable solar arrays are mounted along the Z-axis, either side of the main body of the spacecraft, allowing solar aspect angle to be varied during the cruise phase of the mission while the spacecraft is attached to the solar sail. The solar arrays are small, thus they are stowed against the ± Z-axis faces during launch. The negative X-axis, which faces the Sun during the science phase of the mission, is provided with additional thermal protection. However, all spacecraft faces are required to have sufficient thermal control, as during the cruise phase of the mission the sail attitude may be such as to expose any spacecraft surface to the Sun for a short period of time. The –X face mounts the spacecraft onto the solar sail. By mounting the spacecraft via the –X face we shield the science instruments from the deep space environment until after sail jettison, thus helping to maintain optical surfaces in optimal condition. This configuration however eliminates the potential use of these instruments during the cruise phase of the mission.

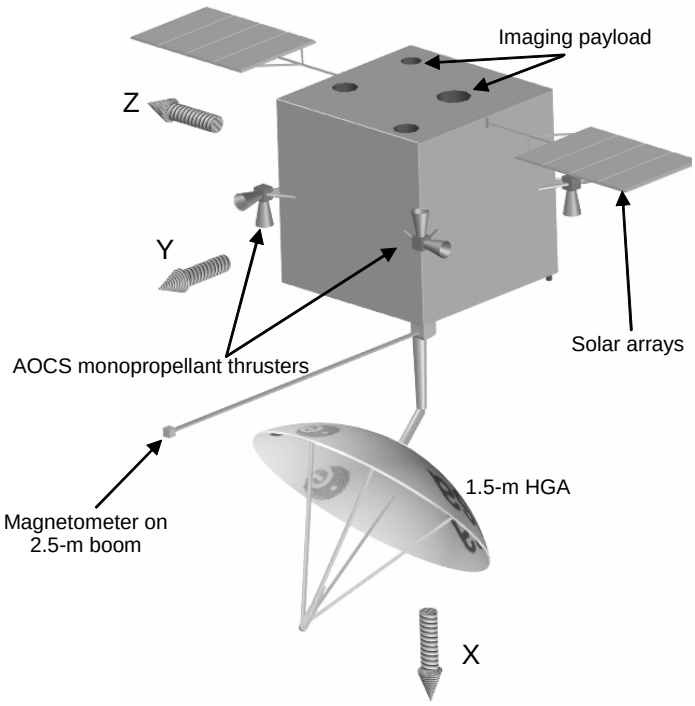

Figure 2 Solar Polar Orbiter preliminary deployed visualization

Variation of Minimum Solar Approach Radius

The spacecraft systems detailed previously were designed for a minimum solar close approach of 0.48 AU. However, from a trajectory perspective an optimal solution can be found by allowing closer solar approaches during transfer. As such, it is important to quantify the effect of varying the solar close approach radius on the spacecraft sub-systems, in order to define this sensitivity. We see in Figure 3 the effect of varying solar approach radius on the wet mass of the spacecraft, without the sail. The design points are intended to provide a good first approximation and as such are suitable for preliminary design analysis. The information in Figure 3 will be coupled with trajectory and sail design information later within this paper in order to fully quantify the effect of varying the minimum solar approach radius.

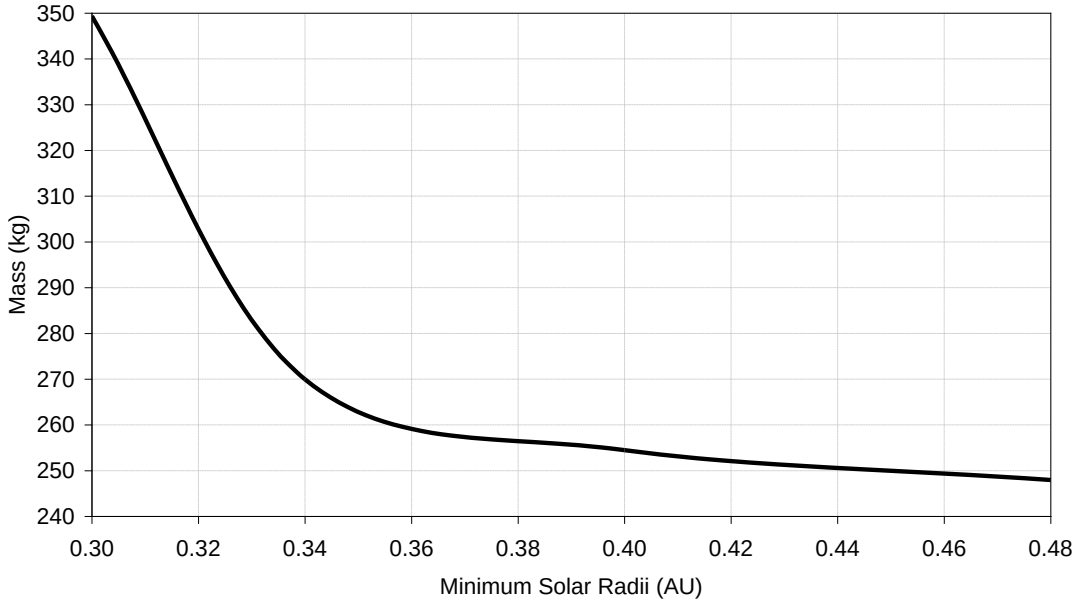

Figure 3 Variation of total spacecraft mass as solar approach thermal limit is varied

Required Sail Slew Rates

From trajectory analysis we note that inclination cranking constitutes the bulk of the transfer trajectory to the solar polar orbit. During the cranking phase the sail pitch is fixed at $\arctan(1/\sqrt{2})$, while the sail clock angle flips from 0 deg to 180 deg.[11] However, it is clear that the sail thrust vector cannot be rotated through ~70.5 deg instantaneously. We thus investigate the effect of varying the sail slew rate in order to quantify requirements on the sail attitude control system. By examination of the locally optimal inclination control law[11] we anticipate that sail slew requirements should be rather low. The rate of change of inclination will approximate a signum function of a cosine curve, with the required sail slew maneuver naturally occurring when the rate of change of inclination is low.

Using a heliocentric trajectory model which includes orbit perturbations due to the terrestrial planets and which models the Sun as a finite uniformly bright disk and the sail as an 85 % efficient reflector, we propagate the orbit cranking sail trajectory for half an orbit revolution. We compare the inclination change over half an orbit against the instant sail slew scenario, allowing investigation of sail slew rates as seen in Figure 4. Figure 4 shows the drop-off, or degradation due to the finite sail slew rate on the rate of change of inclination. We see that at lower sail accelerations the degradation for a given slew rate is increased, while at lower solar radii the degradation is also increased due to the shortened orbit period. We see from Figure 4 that above a sail slew rate of 10 deg per day (10^{-4} deg s^{-1}) the degradation of inclination change is less than 0.5 % at all the accelerations and solar radii considered. We thus define the required sail slew rate as 10 deg per day.

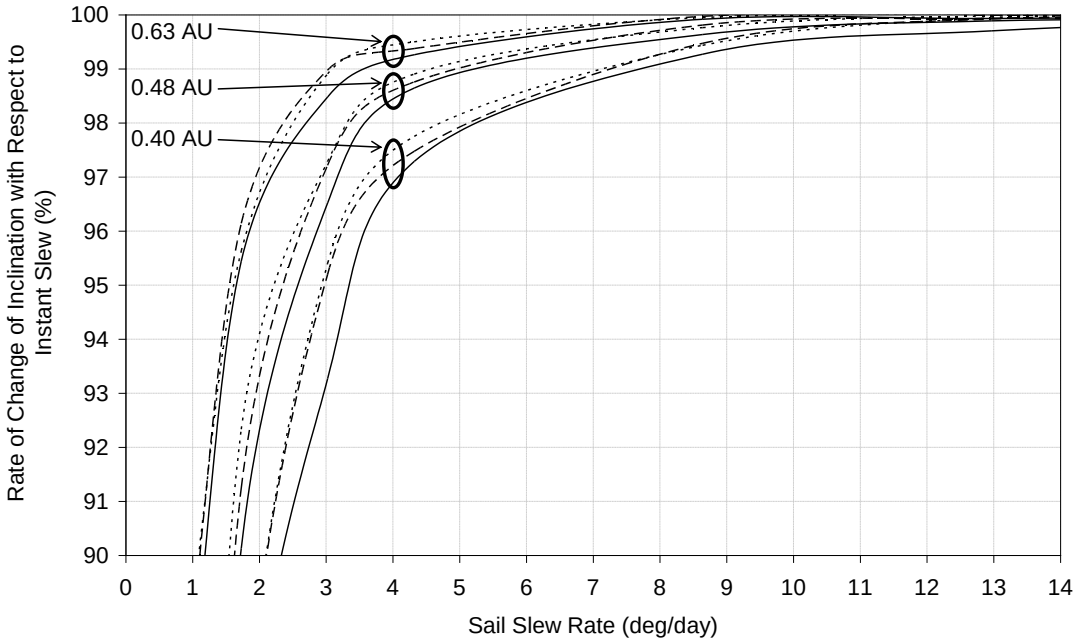

Figure 4 Rate of change of inclination with respect to instant slew scenario. Orbit radius indicated top-left, for three characteristic accelerations at each radii, 0.4 mm s^{-2} (-), 0.5 mm s^{-2} (--) and 0.6 mm s^{-2} (⋯).

Sail Attitude Control

Prior solar sail attitude control system (ACS) studies are limited. Studies for the ST-7 sail estimated that a sail turn rate of 0.01 deg s^{-1} was attainable,[7] significantly higher than the required value of ~10^{-4} deg s^{-1} for the SPO mission. The large moment of inertia of a solar sail and the low-frequency structural dynamics present many unique attitude control challenges. It has been determined that the solar sail required for the SPO mission need not be particularly agile, this significantly simplifies sail ACS hardware design. The optimal ACS solution will likely use the sail structure and mechanisms for attitude control rather than employ a secondary system, which would incur a mass penalty.[8]

Much prior sail design work has base-lined the use a deployable gimbaled boom due to the many apparently attractive features of such a design. However, it has become apparent on detailed study that such a solution is less than optimal due to a lack of full redundancy and control accuracy issues.[8] The use of tip-vanes exclusively is also considered a sub-optimal solution for a variety of reasons.[8] The optimal solution will thus likely employ a combination of systems, thus the inclusion of a secondary system such as μPPT (Pulsed Plasma Thrusters) should not be completely dismissed. In this paper the use of sail tip-vanes is assumed due to the lack of prior ACS studies. Thus an appropriate mass allocation for the sail ACS is included within the sail design, while leaving open the potential for adoption of an alternative ACS.

Recall that the required time to slew ~70.5 deg is approximately 7.05 days, averaging 10 deg per day. However, since the slew maneuver will be symmetrical about the zero clock direction we can model the slew more accurately as acceleration through ~35.2 deg followed by deceleration through ~35.2 deg, each lasting ~3.5 days. If the centre-of-pressure and centre-of-mass are perfectly aligned we find that the sail can accelerate through ~35.2 deg in ~3.5 days with small tip vanes. It is however unlikely that the centre-of-pressure and centre-of-mass will be perfectly aligned due to deployment inaccuracies and sail flexing. Thus we design the tip-vanes such as to compensate for a given centre-of-pressure and centre-of-mass offset, as well as to be able to perform the required slew maneuver in the correct time. The tip vanes are assumed to be isosceles triangles as this minimizes the structural member mass assuming non-inflatable technology is used.

Solar Sail Mass Budget and Definition

Recall from Table 1 that the total sail sub-systems mass is 196 kg. The solar sail mass budget is detailed in Table 5, where it is seen that the mass of the four 14.9 m triangular tip-vanes is 11.4 kg, giving a tip-vane assembly loading of 102.1 g m^{-2}. We note that the wires supplying power and command capability to the boom tips have a total mass of 12.7 kg and form a significant percentage of the total sail mass. While the optimal ACS solution remains to be defined the use of large tip-vanes allows a suitable mass allocation to be defined thus leaving open the potential for adoption of an alternative ACS at some point in the future. The tip-vanes are sized for a centre-of-pressure / centre-of-mass offset error of 0.25 % the sail side length, which corresponds to 0.38 m for this design point. Prior solar sail studies for ST-7 also assumed a centre-of-pressure / centre-of-mass offset error of 0.25 %.[7]

The square sail side length is 153 m, including a 10 × 10 m square central cut-out to allow for sensor field-of-view requirements, at an assembly loading of 8 g m^{-2}. The main sail booms, which support the sail film, are based on a scaling from the Advanced CoilAble booms and a projected near-term solar sail technology roadmap.[12, 13] It is seen in Table 5 that the Sail Stowage Box mass allocation is split into several components, including Primary and Secondary Structure, spacecraft adaptors and the sail deployment equipment. Note the sail stowage and deployment equipment is not jettisoned following sail deployment as would be ideal. This apparent omission actually provides benefits for such an early mission and technology analysis by maintaining a conservative design ideology which increases the sail technology demands above there apparent required level and allows for an increased technology margin. Furthermore, the actual method of jettisoning requires detailed

study to ensure against sail film damage from jettisoned equipment. The “Spacecraft adaptor (carrier side)” detailed in Table 5 provides the mass allocation of the sail jettison mechanism (SJM) on arrival at the target orbit. The mass allocation for the SJM is defined following launch vehicle adaptor methodologies,[14] due to the lack of current SJM designs. The SJM mass allocation is found as 5 % of the spacecraft mass plus a 10 % DMM. THE SJM mass is split 75:25 between the carrier (that is to say the sail) and the spacecraft respectively, thus minimizing spacecraft mass following sail jettison. The SJM, spacecraft side, is allocated within the Mechanisms & Structure sub-system and has mass 3.4 kg. The second adaptor seen in Table 5 corresponds to the launch vehicle adaptor and is defined using similar criteria to the SJM.[14]

The specifics of the solar sail deployment sequence and mechanisms are not defined within this paper as such detail requires specific hardware studies and trades to ensure the optimal sail deployment scenario is identified. The complete solar sail system requires significant further technology development.

Table 5 Solar sail mass breakdown, with scaling laws rounded to one decimal place.

Component		CBE Mass (kg)	DMM (%)	Total Mass (kg)
2 μm CP-1 (Clear Plastic-1) film substrate		66.4	20.0	79.6
0.1 μm Al sail front coating		6.3	5.0	6.6
0.01 μm Cr sail rear coating		1.7	5.0	1.7
Main sail bonding		1.9	10.0	2.0
Main sail booms (65.2 g m^{-1})		28.1	20.0	33.8
Tip vane mass		2.2	12.0	2.6
Tip vane gimbal, motor and housing		8.0	10.0	8.8
Tip-vane control wires		12.1	5.0	12.7
Sail Stowage Box	Primary structure	19.4	10.0	21.3
	Secondary structure	3.2	10.0	3.5
	Deployment and aux. equipment	2.5	10.0	2.8
	Spacecraft Adaptor (carrier side)	9.3	10.0	10.2
	Misc. apparatus, inc. deploy mechanisms	4.3	5.0	4.5
	Launch Adaptor (spacecraft side)	5.6	5.0	5.8
Total		170.7	10.3	195.9

Variation of Sail Systems Technology Parameters

The sail design specifications in Table 5 assume a 2 μm CP-1 film substrate and main sail booms of specific mass 65.2 g m^{-1}. We can examine and quantify the effect of varying these parameters, allowing technology requirement specifications to be more accurately defined. We note that during this trade we fix the main boom specific mass at 50 g m^{-1} when investigating sail film variations and fix the sail film as 2 μm CP-1 while examining main boom specific mass variations. All other parameters in Table 5 vary according to there relationship with the sail size, for example as sail size increases the mass of sail film coatings will also increase.

The variation of boom specific mass linearly alters the sail size and mass. We note from the trajectory analysis later in this paper that the current launch C_3 sets a maximum launch mass of 620 kg, which corresponds to the minimum Soyuz Fregat 2-1b launch mass from Kourou. Increasing the boom specific mass to 150 g m^{-1} we find that the total launch mass, including an ESA system level margin of 20 % is 620 kg. Consequently, to maintain the current mission architecture and time-line, for a 2 μm CP-1 film substrate the maximum boom specific mass is 150 g m^{-1}, giving a sail size of 165 m.

The variation of sail film substrate material will have negligible impact on the sail system mass as most polyimide films have very similar densities. We therefore quantify the effect of varying substrate thickness for CP-1 film and PET film only, as these two substrates represent the opposite ends of the spectrum. Note however that different polyimide films have significantly different thermal properties and as such can impact the allowed minimum solar close approach. We find that the use of 4 μm PET film results in a sail of side length 174 m, while the use of 5 μm CP-1 film results in a sail size of 198 m. Furthermore we note that 1 μm film, such as a commercially available Mylar film, would require a sail side length of only 140 m. Figure 5 shows the effect on sail mass and launch mass as sail substrate thickness is increased. We note that with an upper launch mass limit of 620 kg we can define the required sail film thickness as 3.2–3.4 μm, depending on film material, for a boom specific mass of 50 g m^{-1}. Recall a boom specific mass of 65 g m^{-1} is ultimately selected along with 2 μm CP-1 film.

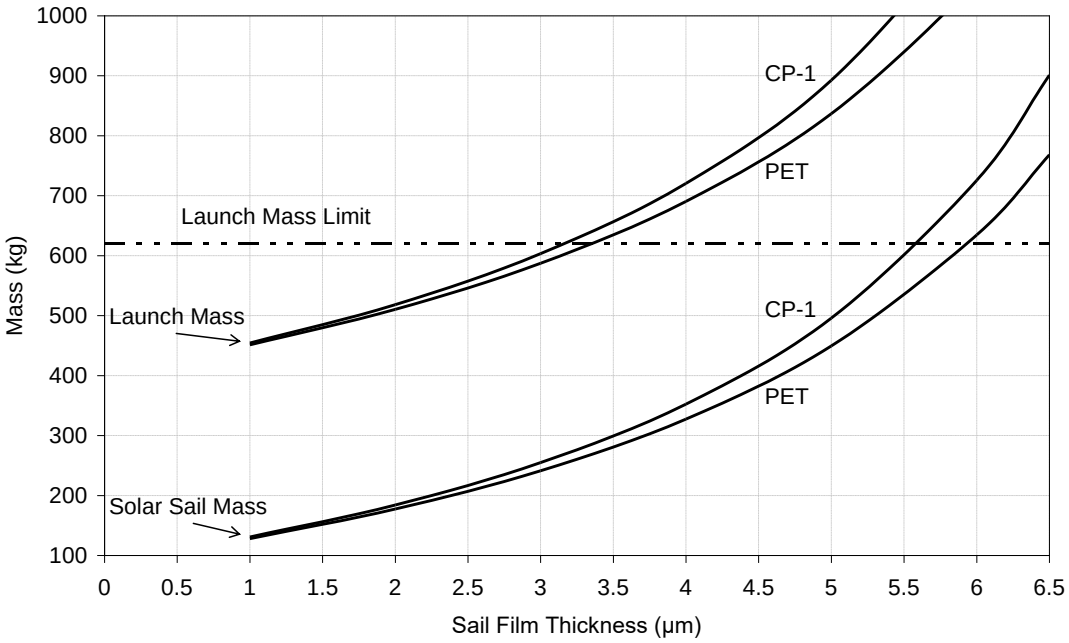

Figure 5 Sail film substrate thickness variation versus sail mass and total launch mass. Each pair of lines corresponds to CP-1 and PET film.

Sail / Spacecraft Separation

Following arrival at the 0.48 AU polar orbit we require to perform a sail separation maneuver prior to initiation of the science phase of the mission. The AOCS propellant budget contains 2.2 kg of hydrazine specifically for sail separation and avoidance maneuvers. On separation from the spacecraft the sail characteristic acceleration increases to 0.98 mm s^{-2} due to the reduction in non-reflective mass. Modeling the separate sail and spacecraft trajectories we find that the separation distance increases at approximately 1 km per minute, assuming no propulsive burn is performed by the spacecraft and that the sail remains passively stable at a setting of zero pitch to the Sun. It is thus possible that the spacecraft may not require the use of its separation and avoidance propellant contingency to initially separate from the sail. However, if we continue to propagate the two trajectories we find that the sail and

spacecraft would go by within 100 km of each other when they both pass over the northern ecliptic pole for the 1st time, again assuming the sail remains passively stable at a setting of zero pitch to the Sun. It is however likely that the sail will begin to tumble sometime after separation from the spacecraft, as it is now uncontrolled. These initial calculations thus suggest that the spacecraft may only require the use of its separation and avoidance propellant contingency to perform sail avoidance maneuvers once the sail begins to tumble but not immediately following sail separation. As sail separation is clearly a key technology issue these initial findings must be further challenged and should be demonstrated in early sail technology demonstration missions.

Launch Configuration and Visualization

Assuming a 2 μm CP-1 film sail substrate and 65 g m^{-1} main sail booms we can investigate the launch configuration and investigate launch fairing compatibility with the Soyuz Fregat 2-1b vehicle. Figure 6 shows that significant volume is available for systems growth and no launch fairing compatibility issues are anticipated. Figure 6 shows the SPO spacecraft on top of the sail deployment box, with the sail booms also shown in their stowed configuration. The main sail booms stow to between one and two percent of there deployed length.[12] The sail film is stowed within the central compartment of the deployment box, revealed only after boom deployment.

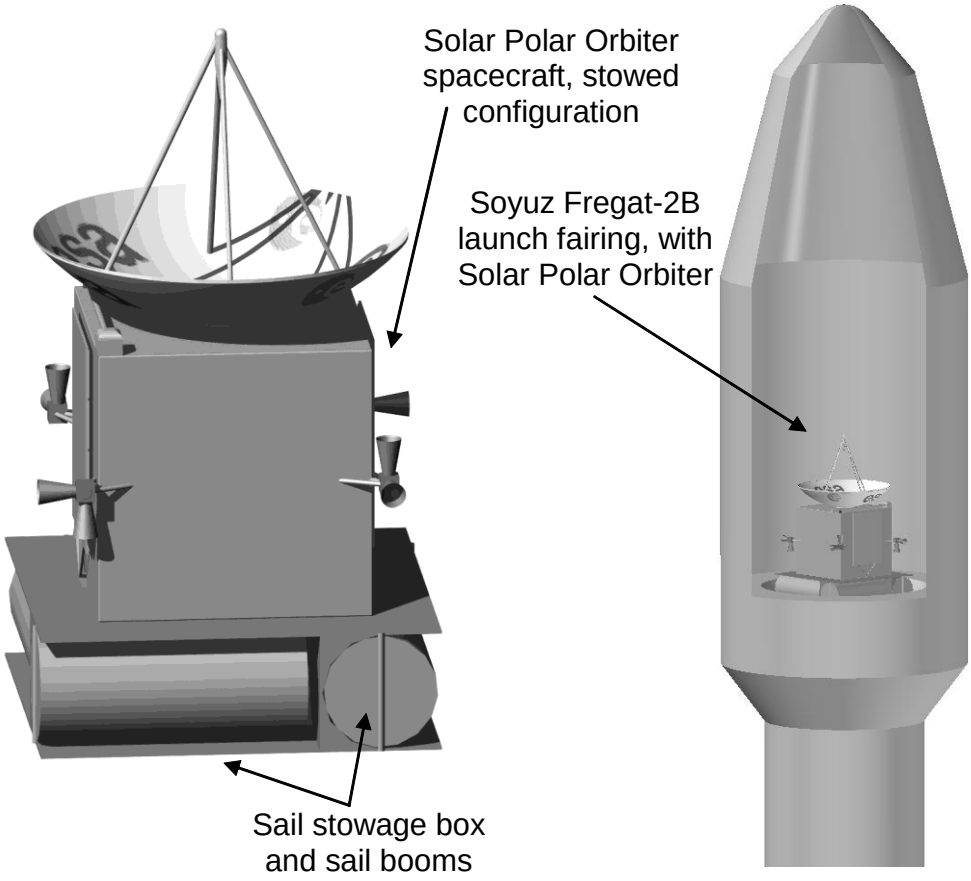

Figure 6 Launch configuration and visualization

Trajectory Analysis

We recall that the target solar polar orbit is defined as inclined at 82.75 deg with a right ascension of 255.8 deg plus 0.014 deg yr^{-1} from J2000, within a standard ecliptic plane reference frame**.** Further, it is desirable that the polar orbit be correctly phased with the Earth to aid mission science returns and avoid solar conjunctions.

Transfers to solar polar orbits have been analyzed in parametric studies by Sauer and briefly by Leipold.[15, 16] After a short optimized spiral to a zero or low inclination circular orbit at the defined minimum solar approach radius, an analytical control law that maximizes the instantaneous rate of change of inclination is utilized to rapidly

increase orbit inclination.[11] Following Sauer,[15] we have adopted a multi-phase approach to the trajectory structure. Closer cranking orbit radii enable more rapid acquisition of polar inclinations, and a third outward spiral phase may be necessary to reach the first few resonant orbits (specifically, N = 1, 2, 3).

The variational equations of the modified equinoctial orbital elements are explicitly integrated using an adaptive step-size, variable order, Adams-Moulton-Bashforth method. The thrust vector direction has been defined by two angles to completely cover the outward hemisphere of allowable orientations. These are the pitch angle, $\alpha \in [0, \pi/2]$, between the sail normal and the Sun-line and the clock angle, $\delta \in [0, 2\pi]$, between the projection of the sail normal and a reference direction onto a plane normal to the Sun-line. A direct, parameter optimization scheme was implemented with the controls specified at discrete nodes at the segment boundaries, equally spaced in time between zero and the terminal time. The controls were characterized across each time segment by linear interpolation between the nodes. As the number of nodes was increased then a close approximation to a continuous profile was achieved. Problems requiring more revolutions, or more rapid control variation (usually for lower accelerations) clearly needed more segments. 50 segments (51 nodes) were considered sufficiently accurate to represent the optimized trajectories in this paper. The trajectory optimization problem is to select the variables that minimize the transfer time (objective function) whilst satisfying the end-point boundary conditions (constraints). This was transcribed to a Non-Linear Programming (NLP) problem, solved using NPSOL 5.0, a Fortran77 package based on Sequential Quadratic Programming (SQP).[17] SQP employs a quasi-Newton approximation to the Karush-Kuhn Tucker conditions of optimality, resulting in a sub-problem of minimizing a

quadratic approximation to the function of Lagrange multipliers incorporating the objective and constraints. Optimality termination tolerance was set to 2×10^{-4}, with the constraint feasibility tolerance at 6.69×10^{-6}. This ensured that final boundary conditions were satisfied to within 1000 km for each position element and to within 0.2 m s^{-1} for each velocity element without performing excessive iterations. NPSOL is a gradient-based, deterministic, local search procedure and therefore requires an initial guess for the cone and clock angle profiles and transfer time that is within the proximity of the actual solution, ensuring a feasible solution is obtained. This was established using homotopy methods to map the initial guess to the final answer.[18]

Approximate Trip Times

Initial, approximate trip times can be obtained by adding the trip times for each of the phases. This however neglects the phasing of the orbits, the Earth ephemeris, and the orientation of the line of nodes of the polar orbit. Note that the line of nodes requirement means that a minimum trip-time opportunity occurs every six months. The launch window can however be considered open at all times through the year, with a trip-time penalty incurred as launch varies from the two optimal start epochs. In general the actual trip-time will be slightly longer than these approximate times, as will be seen later.

It is seen in Figure 7 that the cranking time is very sensitive to the cranking orbit radius, while the curve levels off at higher accelerations. The closer the orbit is to the Sun, the faster the inclination changes. The rate of change of inclination is however constant per integer number of orbit revolutions and is independent of orbit radius, assuming a circular orbit.[11] Low radius orbits have shorter periods and so the

inclination change is effected more rapidly. For a launch C_3 of zero, optimising circular-coplanar transfers from 1 AU to the polar/cranking orbit radius using NPSOL produced inward spiral trip-times. The spiral times were added to the cranking times at the resonant orbit radii and the total 2-phase trip time was found. Cranking at 1 AU or 0.63 AU is tremendously time consuming, thus a 3-phase approach must be adopted to reach these orbits. Further, a 3-phase approach is beneficial for the higher resonance numbers if the close solar orbit thermal loads can be withstood, as seen in Figure 7. Figure 7 concurs with the 0.5 mm s^{-2}, 2-phase transfer to 0.48 AU polar orbit that was previously generated and found to have a duration of order 5 years.[4, 15] It should be noted here that past work does not include positive C_3 launches or take into account Earth ephemeris, orbital orientation and phasing, which will be included later in this paper. A moderate characteristic acceleration of 0.5 mm s^{-2} would require a close cranking orbit of 0.3 AU for a mission duration below 5 years to a $N = 1$ orbit. Using a positive launch C_3 could alleviate this requirement.

Optimized Inward Spirals to Circular Low Inclination orbits at 0.48 AU

In the parametric study conducted by Sauer the inward spiral is optimized to 15 deg inclination before starting the cranking maneuver. If a third outward spiral phase was required then the final 15 deg to reach polar orbit was also optimized. Sauer utilizes a locally optimal inclination control law, which has the drawback of making the generation of fully phased orbits very difficult. It was also noted that the total transfer time is relatively insensitive to initial cranking orbit inclinations above 10 deg.[15] This paper concentrates on the two-phase transfer to a 0.48 AU polar orbit. The effect of optimizing a circle-to-circle inward spiral from 1 AU to 0.48 AU was investigated, for a number of different target orbit inclinations. The optimized inward spiral times

were added to the remaining cranking time necessary to match the inclination to polar orbit. The NPSOL optimization matched the semi-major axis, eccentricity and inclination as constraints. It was found that although the overall saving is less than 6 months, optimizing to 10 – 20 deg is significantly better than for 5 deg. In general, 15 deg seems the optimum value, as was found by Sauer.[15] As the initial cranking orbit inclination is increased beyond these values, many more revolutions are needed and so the optimizer requires more control nodes – placing greater demands on the optimizer.

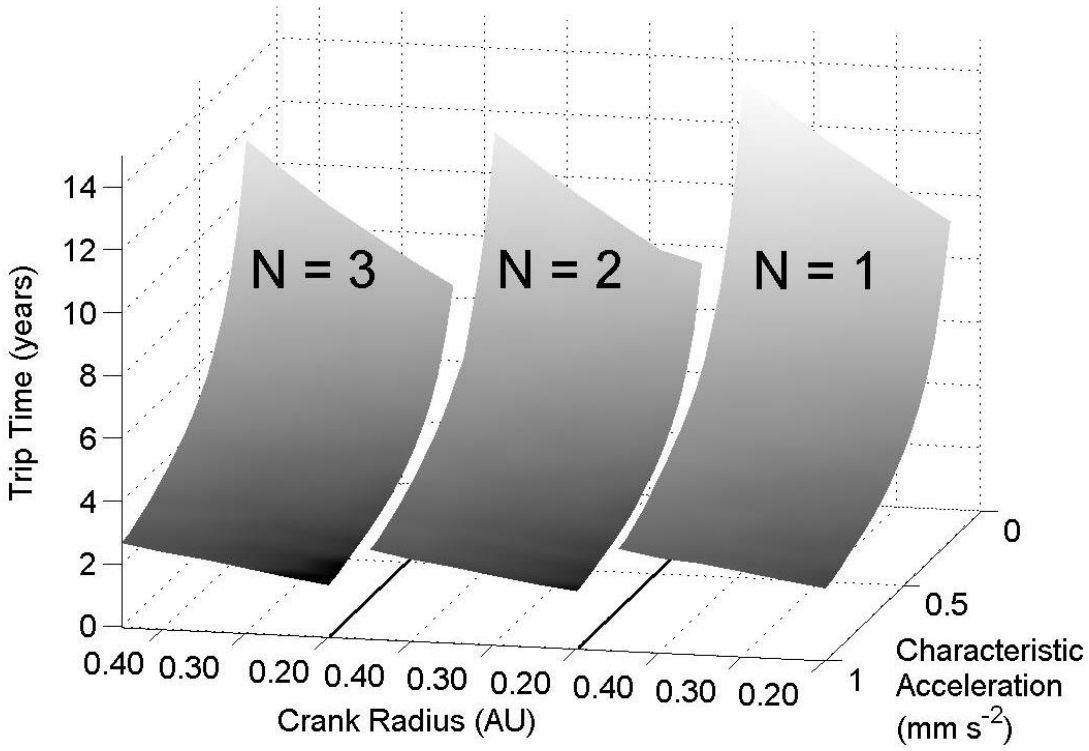

Figure 7 Three-phase total trip times to *N*=1, 2, 3 solar polar orbits

Utilizing Excess Launch Energy

Circular-coplanar optimizations of the inward spiral phase were conducted while increasing the launch C_3 to 40 $km^2\ s^{-2}$, in opposition to the velocity of the Earth. We note that non-zero launch declinations were found to have a significantly adverse effect on sail transfer times and are thus not utilized. 51 control nodes were used. Figure 8 shows the effect of using positive C_3 on the spiral-down time to a 0.48 AU circular orbit over a range of characteristic accelerations. For higher accelerations and higher cranking orbit radii it was found that the curve levels off sooner than for low accelerations and low cranking orbits. There is therefore an increased benefit in using the excess C_3 capability to reach lower cranking orbit radii with low performance sails.

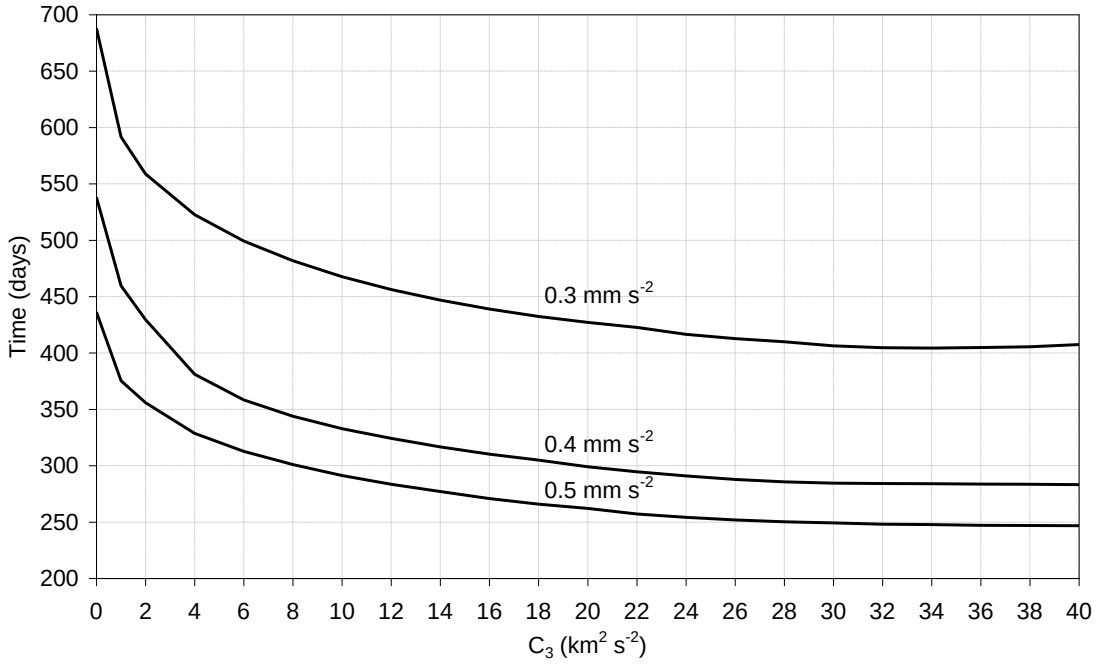

Figure 8 Spiral-in time to circular cranking orbit at a radius of 0.48 AU for characteristic accelerations of 0.3, 0.4 and 0.5 mm s^{-2}, against launch C_3.

We recall that a characteristic acceleration of 0.5 mm s^{-2} was designated earlier within the approximate analysis to reach a 0.48 AU polar orbit with a total transfer time of order 5 years. An attempt was made to reduce the sail performance requirements by using the excess C_3 available, with optimized spiral-in to 15-20 deg inclination. In order to produce an approximate SPO transfer with a trip time of order 5 years, it was found that the characteristic acceleration needed was of order 0.42 mm s^{-2} for a C_3 of 40 km^2 s^{-2}. We note that the Soyuz Fregat 2-1b from Kourou has a minimum launch mass of 620 kg, corresponding to a zero declination positive C_3 of 38.8 km^2 s^{-2}, thus we anticipate that the actual trip time will be slightly in excess of 5 years.

Gravity Assist Option

It is now considered whether any significant benefit can be obtained for the mission from un-powered gravity assists. Multiple gravity assists within the inner solar system tend to be prolonged in duration and can be limited in launch window frequency, especially if considering non-resonant combinations. We therefore anticipate that any benefit will occur through use of a single gravity assist maneuver, probably at Venus, as this will allow for a perihelion inside the Venusian orbit. Use of a Mars or Earth fly-by would result in a high aphelion, which is detrimental to solar sailing. Furthermore, it is envisaged that sail deployment will commence only after the final gravity assist, due to navigational difficulties with such a large structure and inaccurate pointing control due to sail flexing. The delayed deployment of the sail will avoid the need for accurate sail navigation and control during the gravity assist, but would require some additional propellant on the spacecraft bus for trajectory correction maneuvers, probably within the AOCS hydrazine budget. Furthermore, the

significant level of available launch C_3 means that sail deployment prior to a Venus fly-by would have negligible impact on the duration of this transfer.

Launching on 27 December 2017 we perform a 2883 km Venus fly-by 142 days later on 18 May 2017, placing the un-deployed solar sail on a 0.73 AU × 0.52 AU × 18 deg orbit. Following sail deployment on this orbit the primary trajectory goal is to circularize the orbit at 0.48 AU. During orbit circularization it was found that the orbit inclination can be increased slightly with no degradation on the circularization goal, so that the sail arrives on an orbit of 0.48 AU × 0.48 AU × 22.32 deg after 195 days, 337 days after launch. Note that this trajectory analysis was performed using A^nD blending, a method which blends locally optimal control laws and allows a more rapid analysis than traditional methods.[19 - 22] Each control law is prioritized by consideration of how efficiently it will use the solar radiation pressure and how far each orbital element is from its target value. It has been demonstrated that trajectories found with A^nD blending are very similar or better than those found using traditional trajectory optimization methods.[21, 22] On arrival at the circular 0.48 AU orbit the locally optimal inclination control law is once again used to raise the orbit inclination. The complete orbit transfer duration is 4.13 years from the Venus fly-by, giving a total flight time from launch of 4.52 years. An un-powered Venus gravity assist can thus provide a saving of 0.4 years for a reduced sail acceleration of 0.4 mm s^{-2}. Thus, the use of a Venus gravity assist can as anticipated offer some potential benefits over a conventional mission profile, although the saving in transfer time and sail performance appear modest. This option was not selected as the reference trajectory as at this stage of analysis it was felt a conservative estimate of solar sail technology requirements was required. Moreover, the technological challenge of stowing a sail

for approximately 150 days in the space environment prior to an autonomous deployment at 0.6 AU slant range was considered significant, furthermore it was considered problematical to emulate in a technology demonstration mission in-order to reduce the risk. Note, the slight reduction in sail size would be somewhat offset by the increase in required spacecraft mass due to the increase in propellant mass; this was not modeled here. It is noted however that a Venus gravity assist provides some benefit and thus remains a valid option during future analysis.

Fast Mission Option

An alternative mission option would be to employ a 3 phase strategy, to reach a 0.48 AU polar orbit more rapidly. The cranking orbit was set at 0.30 AU, with the minimum solar radius also constrained at this distance. A slight increase in the characteristic acceleration to 0.5 mm s^{-2}, with an increase in the mass of the thermal sub-system, means the sail side length is of order 200 m. The increased launch mass results in a maximum available C_3 of 27.9 km^2 s^{-2}. The optimized, positive C_3 inward spiral time (coplanar) was found to be 320 days. The orbit then cranks up to 82.75° in 706 days. The third phase was then optimized to spiral outwards from the cranking orbit to the final orbit radius of 0.48 AU, in 110 days. The total trip time to polar orbit was 3.11 years, for this fast-mission option, however savings could be made by removing the coplanar transfers. Figure 9 shows the entire 3 phases of the trajectory. While this option offers a significant time saving, the increased risk and cost of a prolonged stay at 0.3 AU, coupled with the increase in sail size meant this option was considered sub-optimal.

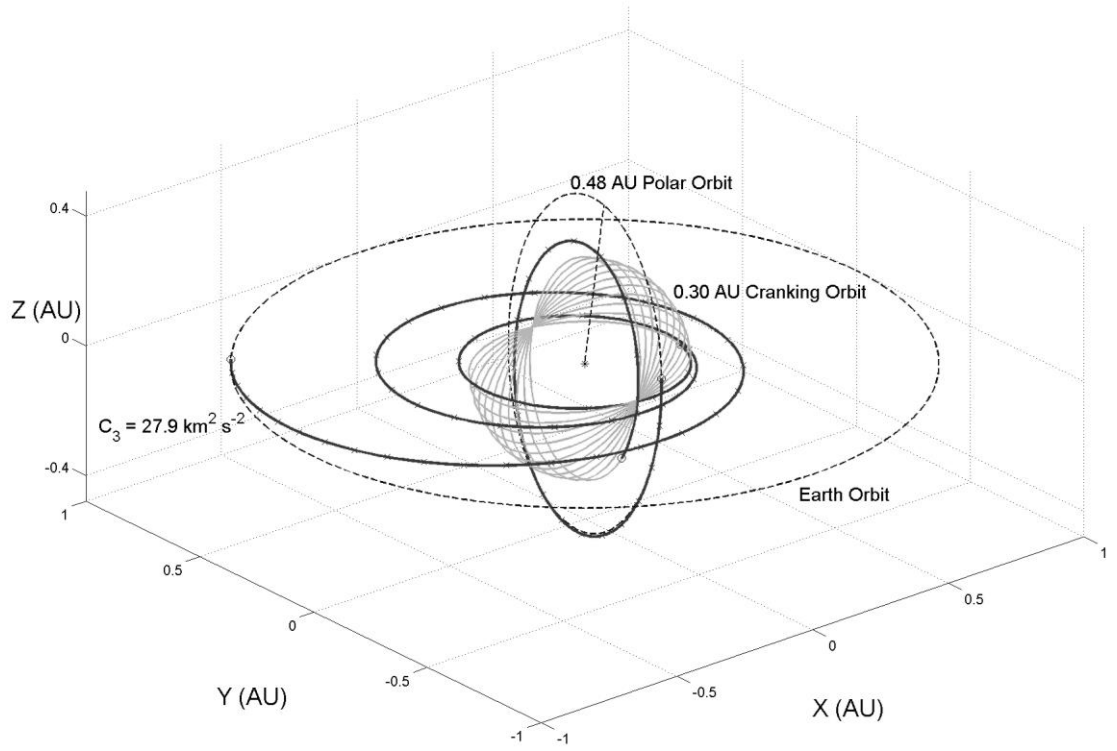

Figure 9 0.5 mm s^{-2} fast mission solar polar orbit trajectory

Reference Trajectory

The problem of obtaining the correct phasing at arrival on the solar polar orbit was deemed to be best tackled by selecting an arrival date and position on the solar polar orbit that is correctly phased with the Earth. Then the analytical cranking control law was used to propagate the trajectory over a negative time-span, thus reducing inclination. The resultant orbital elements were then used as the initial conditions for a further reverse optimization, back to Earth. Integration over a negative time-span has been used for low-thrust trajectory optimization in the past, for example the early SMART-1 mission studies,[23] however it has not previously been used to generate correctly phased solar polar orbits. The arrival position was selected as the north solar pole, with the Earth-Sun-sail angle at 90 deg. The Earth was found to be at this azimuth angle in the early hours of 07 June 2015 (Universal Time), which was thus

defined to be the SPO arrival date, allowing for an approximate Earth departure date in 2010.

For a characteristic acceleration of 0.42 mm s^{-2}, the spacecraft is launched on 16 May 2010, with a positive launch excess energy of C_3 = 38.84 km^2 s^{-2}, the maximum available from a Soyuz Fregat 2-1b from Kourou. A constraint was placed on the minimum solar radius of 0.48 AU. The optimal sail spiral down to the cranking orbit is inclined to 14.42 deg in 457.5 days. This intermediate orbit has a semi-major axis of 0.4828 AU and an eccentricity of 0.0762 AU. The analytical cranking then takes place from 17 August 2011, raising the inclination to 82.75 deg at a circular 0.48 AU solar polar orbit in 1390 days. The complete trajectory is shown in Figure 10, where the total transfer duration is 5.06 years. The maximum Earth-spacecraft distance is 1.654 AU, which is well within the maximum cruise mode slant range of the TT&C system, Table 3.

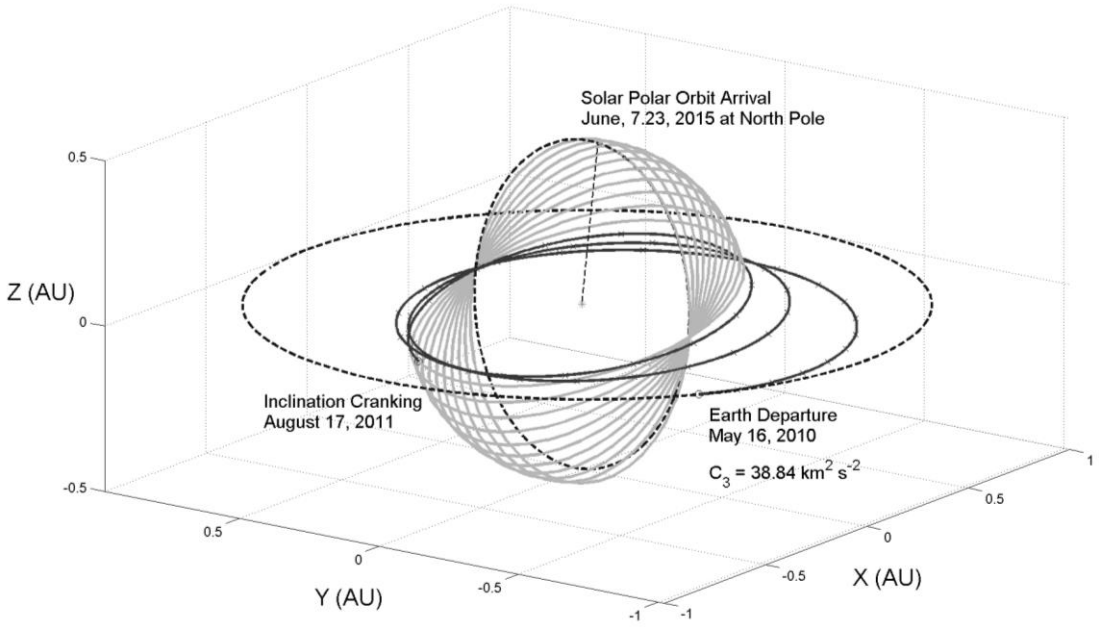

Figure 10 0.42 mm s^{-2} reference mission solar polar orbit trajectory

On arrival at the target orbit the sail is jettisoned as discussed earlier. A high fidelity trajectory model was used to propagate the solar polar orbit over 2 years with perturbations from the all the planets out to and including Saturn. As expected the orbital elements deviate by a negligible amount from the nominal values, with the maximum Earth-spacecraft distance found to be 1.45 AU, which is within the maximum science mode and space weather mode slant ranges of the TT&C system, Table 3.

Competing Propulsion Options

The delivery of a spacecraft into a solar polar orbit is a challenging mission concept, as has been seen by the inability of the Solar Orbiter mission to attain a solar polar orbit with current SEP technology.[3] The velocity change requirement to attain a solar polar orbit with chemical propulsion is of order 42 – 56 km s^{-1}, depending on N. Thus, chemical propulsion alone cannot provide a solar polar orbit and we must consider the use of gravity assist maneuvers. In order to reach an aphelion within the Earth's orbit we must restrict fly-bys to the terrestrial planets. However, the small mass of these planets means that the time to a polar orbit is unrealistically high.

The elimination of both conventional SEP and chemical propulsion as competing systems restricts our analysis to new and novel propulsion systems, such as nuclear electric propulsion (NEP), radioisotope electric propulsion (REP) or Mini-Magnetospheric Plasma Propulsion (M2P2). It is expected that any NEP system will require a large launch vehicle due to the inherent nature of the system, thus eliminating the use of a Soyuz-Fregat vehicle. Meanwhile, the use of a REP system

would require extremely advanced radioisotope power sources to compete with solar power. For example, if we replace the solar arrays with an advanced radioisotope power systems (ARPS) of the same mass we would require a power density of 13.5 W kg^{-1}. However, if we add in a 5 kW electric propulsion system the solar array mass rises to just under 80 kg, for a total array surface area of 20 m^2, which would require an ARPS specific mass of over 50 W kg^{-1} in order to match the power mass budgets. M2P2 could potentially provide the required change in velocity needed to attain a true solar polar orbit. This concept is akin to solar sails, but has the advantage of not requiring large structures to be deployed. The drawback to this propulsion method is that the magnetic field generating system mass may be quite high. The lack of viable competing propulsion systems serves to highlight the potential of solar sailing for a solar polar mission concept. We thus conclude that solar sailing offers great potential for this mission concept and indeed may represent the first useful deep space application of solar sail propulsion.

Variation of Minimum Solar Approach Radius

We see from Figure 3 and Figure 7 the effect of varying the minimum solar approach radius on spacecraft mass and transfer duration to the polar orbit. Using the extensive parametric trajectory data set generated we can estimate sail characteristic acceleration requirements for a given minimum solar approach radius and trip time to the 0.48 AU solar polar orbit, for a launch C_3 of zero. Thus, by combining sail characteristic acceleration requirements, spacecraft mass and minimum solar approach radius we can quantify the global effect of varying the minimum solar approach radius. During this trade we assume 2 μm CP-1 sail film substrate and 50 g m^{-1} main

sail booms, along with the sail design scaling discussed earlier and the spacecraft masses in Figure 3.

Figure 11 shows the effect of varying the minimum solar approach radius on sail side length. We note that despite the significantly increased spacecraft mass required to survive such a severe thermal environment a minimum sail side length occurs for a minimum solar approach radius of 0.33 – 0.34 AU depending on desired mission transfer duration. A 5-year transfer trajectory can thus be attained with a sail of side length 150 m and minimum solar approach radius 0.34 AU. A similar trade was performed for launch mass versus minimum solar approach radius. It was found that the minimum launch mass varied from 0.34 – 0.36 AU, for trip time 3 – 5 yrs respectively. Thus, the minimum sail size does not provide for a minimum launch mass. However, the launch mass of the minimum sail size configuration for a 5 year transfer was less than 620 kg, the lower bound limit of the Soyuz Fregat 2-1b from Kourou and as such optimizing the launch mass can be considered secondary to sail size optimization. The use of a positive launch energy within this paper allows for a reduction in sail size towards the same value as an optimal (minimum sail size) architecture $C_3 = 0$ launch.

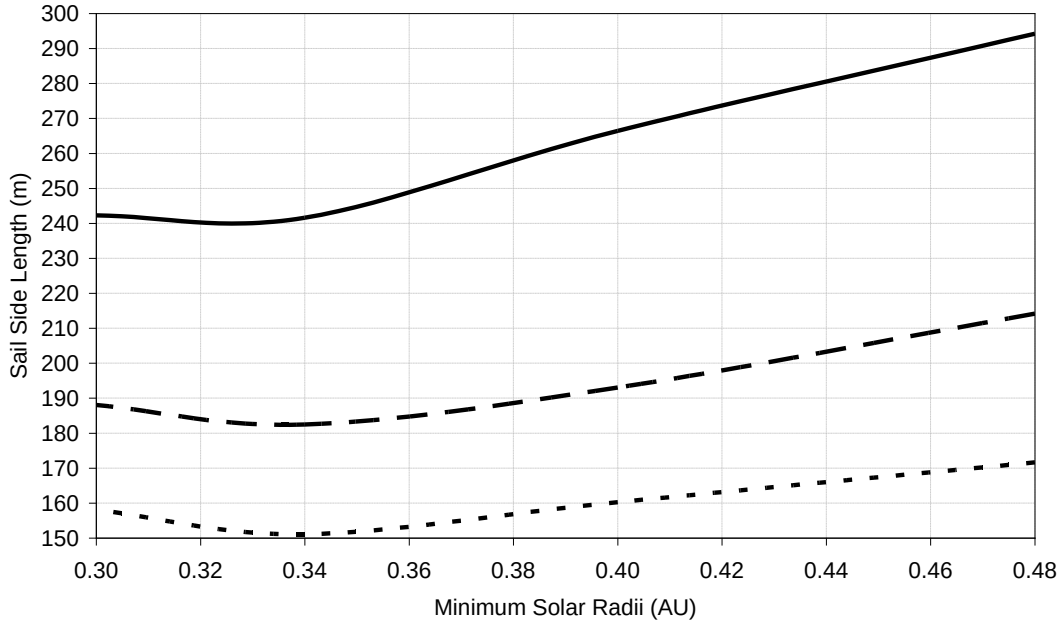

Figure 11 Minimum solar radius versus sail size for 5-yr (···), 4-yr (--) and 3-yr (-) trip times to 0.48 AU solar polar orbit

Conclusions

A Solar Polar Orbiter mission concept has been presented as a Technology Reference Study. The mission utilizes a Soyuz Fregat 2-1b launched from Kourou. The low launch mass of 532 kg, including margins allows for maximum launch energy to be used, providing the sail with an initial Earth C_3 in excess of 38 km^2 s^{-2}. The use of positive C_3 and a single Venus fly-by were shown to reduce the sail performance requirements, though the later was not adopted. The mission primary propulsion system was defined a priori as solar sailing and we find that the required sail is 153 × 153 m for the baseline 5-year transfer mission scenario. However, sail size can be reduced through closer solar approaches despite the significantly increased spacecraft mass required to survive the increasingly hostile environment at low solar radii. Optimal close approach radii were presented to minimize launch mass and sail size,

all of which were above 0.3 AU. A comprehensive trajectory study was completed and, for the first time, a trajectory generated to an accurately phased and positioned orbit.

The solar sail and spacecraft technology requirements have been addressed. The sail requires advanced boom and new thin-film technology. The sail was found to be at a low technology readiness level requiring significant further effort. By contrast the spacecraft requirements were found to be minimal, as the spacecraft environment is relatively benign in comparison with other currently envisaged missions. However, the spacecraft design was found to vary in some key areas from a non-sail delivered mission due to, for example, sail pointing accuracy limiting the communications system to X-band and below. Overall, the technology requirements for a Solar Polar Orbiter mission have been clearly identified.

Acknowledgments

This study was conducted under contract “ESTEC 16534/02/NL/NR: Technical Assistance in the Study of Science Payloads Transported Through Solar Sailing". The authors thank Henry Garrett of the Jet Propulsion Laboratory of the National Aeronautics and Space Administration (JPL-NASA) for his input into the study of potential cruise phase science issues regarding sail interactions with the space environment.

References

[1] Lyngvi, A., Flakner, P., Renton, D., v.d.Berg, M.L., Peacock, A., "Technology Reference Studies", IAC-04-U.1.06, Electronic Proceedings of 55th International Astronautical Congress, Vancouver, October 2004.

[2] European Space Agency Science and Technology, "Ulysses", URL: http://sci.esa.int/science-e/www/area/index.cfm?fareaid=11 [citied 12 June 2004]

[3] European Space Agency Science and Technology, "Solar Orbiter", URL: http://sci.esa.int/science-e/www/area/index.cfm?fareaid=45 [citied 12 June 2004]

[4] Goldstein, B., Buffington, A., Cummings, A.C., Fisher, R., Jackson, B.V., Liewer, P.C., Mewaldt, R.A., Neugebauer, M., "A Solar Polar Sail Mission: Report of a Study to Put a Scientific Spacecraft in a Circular Polar Orbit about the Sun", Proceedings of MTG: SPIE International Symposium on Optical Science, Engineering and Instrumentation, San Diego, California, July 1998.

[5] Balthasar, H., Stark, D., and Wöhl, "The Solar Rotation Elements i and Ω Derived from Recurrent Single Sunspots," Astronomy and Astrophysics, Vol. 174, pp. 359-360, 1987.

[6] European Space Agency Science and Technology, "BepiColombo", URL: http://sci.esa.int/science-e/www/area/index.cfm?fareaid=30 [citied 12 June 2004]

[7] Wie, B., "Sail Flatness, Attitude, and Orbit Control Issues for an ST-7 Solar Sail Spacecraft", NASA SSTWG FY01, Solar Sail Technical Interchange Meeting, NASA Goddard Space Flight Center, 2001.

[8] Murphy, D., Wie, B., "Robust Thrust Control Authority for a Scalable Sailcraft", AAS 04-285, Electronic Proceedings of 14th AAS/AIA Space Flight Mechanics Conference, Maui, Hawaii, 2004

[9] Garrett, H., Wang, J., "Simulations of Solar Wind Plasma Flow Around A Simple Solar Sail", Proceedings of the 8th Spacecraft Charging Technology Conference, Ed. R. Suggs, MSFC, Huntsville, Alabama, October 2003.

[10] Spectrolab Photovoltaic Data Sheet, available from www.spectrolab.com [citied 12 June 2004]

[11] McInnes, C.R., "Solar Sailing: Technology, Dynamics and Mission Applications", Springer-Praxis, Chichester, 1999.

[12] Murphy, D.M., Murphey, T.W., "Scalable Solar-Sail Subsystem Design Concept", Journal of Spacecraft and Rockets, Vol. 40, No. 4, pp. 539-547, 2003.

[13] Macdonald, M., McInnes, C.R., "A Near-Term Roadmap for Solar Sailing", IAC-04-U.1.09, Electronic Proceedings of 55th International Astronautical Congress, Vancouver, October 2004.

[14] Wertz, J.R., Larson, W.J. (Eds.), "Space Mission Analysis and Design", Kluwer Academic Publishers Group, Dordrecht, Section 11.6, pp. 459-497, 1999.

[15] Sauer, C. G., Jr., "Solar Polar Trajectories for Solar-Polar and Interstellar Probe Missions," AAS 99-336, Proceedings of AAS/AIAA Astrodynamics Specialists Conference, Girdwood, Alaska, August 1999.

[16] Leipold, M., "Solar Sail Mission Design," PhD Dissertation, DLR Köln, February 2000.

[17] Hughes, G.W., McInnes, C.R., "Small Body Encounters Using Solar Sail Propulsion", Journal of Spacecraft and Rockets, Vol. 41, No. 1, pp 140-150, 2004.

[18] Hughes, G.W., "A Realistic, Parametric Compilation of Optimised Heliocentric Solar Sail Trajectories", PhD Dissertation, Department of Aerospace Engineering, University of Glasgow, June 2005.

[19] Macdonald M., McInnes C. R., "Realistic Earth Escape Strategies for Solar Sailing", Journal of Guidance, Control, and Dynamics, Vol. 28, No. 2, pp 315 – 323, 2005.

[20] Macdonald M., McInnes C. R., "Analytical Control Laws for Planet-Centred Solar Sailing", Journal of Guidance, Control, and Dynamics, Vol. 28, No. TBC, pp. TBC, 2005.

[21] Macdonald M., McInnes C. R., Dachwald, B., "Analytical Control Laws for Heliocentric Solar Sail Orbit Transfers", Submitted to Journal of Spacecraft and Rockets, April 2005.

[22] Macdonald M., "Analytical Methodologies for Solar Sail Trajectory Design", PhD Dissertation, Department of Aerospace Engineering, University of Glasgow, May 2005.

[23] Schoenmaekers, J., Pulido, J., Jehn, R., "SMART-1 Mission Analysis: Moon Option", ESA Report S1-ESC-RP-5001, Issue 1, Noordwijk, September 1998.